Ji et al. Journal of Biomedical Science (2017) 24:44
DOI 10.1186/s12929-017-0352-x

科 技 部 Ministry of Science and Technology
The cost of publication in Journal of Biomedical Science is borne by the Ministry of Science and Technology, Taiwan.

Journal of Biomedical Science

RESEARCH Open Access

PA-6 inhibits inward rectifier currents carried by V93I and D172N gain-of-function $K_{IR}2.1$ channels, but increases channel protein expression

Yuan Ji[1], Marlieke G. Veldhuis[1], Jantien Zandvoort[1], Fee L. Romunde[1], Marien J. C. Houtman[1], Karen Duran[2], Gijs van Haaften[2], Eva-Maria Zangerl-Plessl[3], Hiroki Takanari[1], Anna Stary-Weinzinger[3] and Marcel A. G. van der Heyden[1*]

Abstract

Background: The inward rectifier potassium current I_{K1} contributes to a stable resting membrane potential and phase 3 repolarization of the cardiac action potential. *KCNJ2* gain-of-function mutations V93I and D172N associate with increased I_{K1}, short QT syndrome type 3 and congenital atrial fibrillation. Pentamidine-Analogue 6 (PA-6) is an efficient (IC_{50} = 14 nM with inside-out patch clamp methodology) and specific I_{K1} inhibitor that interacts with the cytoplasmic pore region of the $K_{IR}2.1$ ion channel, encoded by *KCNJ2*. At 10 μM, PA-6 increases wild-type (WT) $K_{IR}2.1$ expression in HEK293T cells upon chronic treatment. We hypothesized that PA-6 will interact with and inhibit V93I and D172N $K_{IR}2.1$ channels, whereas impact on channel expression at the plasma membrane requires higher concentrations.

Methods: Molecular modelling was performed with the human $K_{IR}2.1$ closed state homology model using FlexX. WT and mutant $K_{IR}2.1$ channels were expressed in HEK293 cells. Patch-clamp single cell electrophysiology measurements were performed in the whole cell and inside-out mode of the patch clamp method. $K_{IR}2.1$ expression level and localization were determined by western blot analysis and immunofluorescence microscopy, respectively.

Results: PA-6 docking in the V93I/D172N double mutant homology model of $K_{IR}2.1$ demonstrated that mutations and drug-binding site are >30 Å apart. PA-6 inhibited WT and V93I outward currents with similar potency (IC_{50} = 35.5 and 43.6 nM at +50 mV for WT and V93I), whereas D172N currents were less sensitive (IC_{50} = 128.9 nM at +50 mV) using inside-out patch-clamp electrophysiology. In whole cell mode, 1 μM of PA-6 inhibited outward I_{K1} at −50 mV by 28 ± 36%, 18 ± 20% and 10 ± 6%, for WT, V93I and D172N channels respectively. Western blot analysis demonstrated that PA-6 (5 μM, 24 h) increased $K_{IR}2.1$ expression levels of WT (6.3 ± 1.5 fold), and V93I (3.9 ± 0.9) and D172N (4.8 ± 2.0) mutants. Immunofluorescent microscopy demonstrated dose-dependent intracellular $K_{IR}2.1$ accumulation following chronic PA-6 application (24 h, 1 and 5 μM).

Conclusions: 1) *KCNJ2* gain-of-function mutations V93I and D172N in the $K_{IR}2.1$ ion channel do not impair PA-6 mediated inhibition of I_{K1}, 2) PA-6 elevates $K_{IR}2.1$ protein expression and induces intracellular $K_{IR}2.1$ accumulation, 3) PA-6 is a strong candidate for further preclinical evaluation in treatment of congenital SQT3 and AF.

Keywords: I_{K1}, $K_{IR}2.1$, Atrial fibrillation, Short QT syndrome, Drugs, PA-6, Trafficking

* Correspondence: m.a.g.vanderheyden@umcutrecht.nl
[1]Department of Medical Physiology, Division of Heart and Lungs, University Medical Center Utrecht, Yalelaan 50, 3584 CM Utrecht, The Netherlands
Full list of author information is available at the end of the article

Background

In the heart, inward rectifier potassium currents (I_{K1}) contribute to stabilization of the resting membrane potential of contractile cardiomyocytes and participate in the final phase of repolarization of the action potential [1]. Gain-of-function mutations in the *KCNJ2* gene, that encodes $K_{IR}2.1$ protein underlying I_{K1}, associate with ventricular (short QT syndrome type 3 (SQT3)) and atrial (congenital atrial fibrillation (AF)) phenotypes. D172N and K346T are linked to SQT3, whereas V93I associates with congenital AF [2–4]. E299V and M301K have been linked to both SQT3 and AF [5, 6].

Congenital SQT syndrome is diagnosed in the presence of a QTc interval equal or less than 330 ms, and may be diagnosed at a QTc of less than 360 ms when other conditions apply, like a pathologic mutation or a family history of SQT [7]. Congenital SQT can either be caused to excessive repolarization capacity (SQT1-3), or due to decreased depolarization capacity (SQT4-7), and is associated with high risk for sudden cardiac death and therefore implantable cardioverter-defibrillator (ICD) implantation is indicated [8, 9]. However, pharmacotherapy may be beneficial in patients that are unsuitable for ICD therapy (e.g. young children), those that refuse ICD implantation or for bridging the time to ICD implantation [10]. Some drugs are indeed able to inhibit currents produced by $K_v11.1$, $K_V7.1$ and $K_{IR}2.1$ channels bearing gain-of-function mutations associated with SQT1, SQT2 and SQT3, respectively [11–14].

AF is associated with increased risk for stroke and heart failure [15]. Action potential lengthening drugs, e.g. targeting the delayed rectifier (I_{Kr}), or drugs increasing atrial fibrillation cycle length (sodium current (I_{Na}) blockers), have the potential to counteract AF [16]. Inhibition of the acetylcholine activated inward rectifier potassium current (I_{KAch}) channel, closely related to the I_{K1} channel, has been proposed as an effective treatment in AF [17]. Also I_{K1} inhibiting compounds, like chloroquine, display anti-AF activity in animal models [18, 19].

We have developed a new I_{K1} inhibiting compound, named PA-6, recently [20]. After crossing the plasma membrane, PA-6 can enter the I_{K1} channel from the cytoplasmic side, will bind to the channel by lipophilic interactions and hydrogen bonds to residues E224, D259 and E299, and subsequently inhibits inward and outward potassium current with an IC_{50} in the low nanomolar range [20]. Recently, we demonstrated that PA-6 lengthens action potential duration, atrial fibrillation cycle length and cardioverts goats with rapid pacing induced AF to sinus rhythm [20, 21]. Interestingly, some ion channel inhibitors are able to increase channel expression [20, 22], or restore normal plasma membrane expression of trafficking defective mutant channels [23–25], probably by stabilizing the channel structure as a result of their direct interaction. Also PA-6 is able to increase expression of wild-type (WT) $K_{IR}2.1$ channels [20].

We hypothesized that PA-6 inhibits I_{K1} channels that are formed by gain-of-function $K_{IR}2.1$ channel proteins and thus can be considered as a candidate drug in treating SQT3 and congenital AF.

Methods

Molecular modelling

Docking of compound PA-6 was conducted using the previously constructed closed state homology model of the human $K_{IR}2.1$ channel [20]. In silico mutations of residues V93I and D172N were generated with SwissPdbViewer [26]. Compound PA-6 was generated as described previously [20]. The docking program FlexX (part of the LeadIT software package version 2.0.1 (BioSolveIT GmbH, St Augustin, Germany) was used for docking. The binding site was specified selecting the carboxylic acids of the Glu224 residues from all four subunits. The radius of the binding site was set to 20 Å. Default settings of FlexX were applied for protonation and torsion angles. The ChemScore scoring function of FlexX was applied and the top 10 docking solutions were saved for analysis.

KCNJ2 constructs

Mutations V93I and D172N were engineered into a human *KCNJ2*-pcDNA3 expression construct [27], using the QuikChange II XL Site-Directed Mutagenesis Kit (Stratagene, La Jolla, CA) and custom designed primers. The presence of the introduced mutations was confirmed by Sanger sequencing.

Patch-clamp electrophysiology

HEK293T cells were transfected with WT, V93I or D172N constructs together with a GFP expression construct to enable detection of transfected cells. Inside-out patch clamp measurements were made using a HEKA EPC-10 Double Plus amplifier controlled by PatchMaster 2.10 software (HEKA, Lambrecht/Pfalz, Germany) at 21 °C. To record WT, V93I and D172N $K_{IR}2.1$ currents, inside-out patch-clamp measurements were performed using a ramp protocol ranging from −100 to +100 mV in 5 s from a holding potential of −40 mV. Excised patches were placed in close proximity to the inflow region of the perfusion chamber. Bath solution contained 125 mM KCl, 4 mM EDTA (2K), 7.2 mM K_2HPO_4, 2.8 mM KH_2PO_4, pH 7.20/KOH. Pipette solution contained 145 mM KCl, 1 mM $CaCl_2$, 5 mM HEPES, pH 7.40/KOH. Measurements were started following washout of polyamines/Mg^{2+} from the channel pore observed by the disappearance of current rectification. For IC_{50} curves, fractional block at −80 and +50 mV was determined by dividing current levels

obtained with PA-6 containing solutions by current levels of control traces recorded in the absence of PA-6.

Whole cell patch clamp measurements were done as described before [28] using an AxoPatch 200B amplifier controlled by pClamp9 software (Molecular devices, Sunnyvale, CA, USA) at 21 °C. Whole cell $I_{KIR2.1}$ measurements were performed by applying 1 s test pulses ranging between −120 and +30 mV, in 10 mV increments, from a holding potential of −40 mV, and with series resistance compensation of at least 70%. Steady state current at the end of the pulse was normalized to cell capacitance and plotted versus test potential (corrected for liquid junction potential). Extracellular solution contained 140 mM NaCl, 5 mM KCl, 1 mM $CaCl_2$, 1 mM $MgCl_2$, 6 mM glucose, 17.5 mM $NaHCO_3$, 15 mM HEPES, pH 7.4/NaOH. Pipette solution contained 125 mM potassium gluconate, 10 mM KCl, 5 mM HEPES, 5 mM EGTA, 2 mM $MgCl_2$, 0.6 mM $CaCl_2$, 4 mM Na_2ATP, pH 7.20/KOH.

PA-6 (Fig. 1a) was custom synthesized by Endotherm GmbH (Saarbrücken, Germany).

Western blot

HEK293T cells were grown in 60 mm culture dishes containing 3 mL DMEM supplemented with 10% FCS, L-Glutamine and Pen-Strep, and transfected using linear polyethylenimine (PEI) (PolysciencesInc, Eppelheim, Germany) as described earlier [29]. Cell lysates were prepared in buffer D (20 mM HEPES, 125 mM NaCl, 10% glycerol, 1 mM EDTA, 1 mM EGTA, 1 mM dithiothreitol, and 1% Triton X-100, pH 7.6, supplemented with 1 mM PMSF and 10 μg/mL aprotinin). 20 μg protein lysate was separated by 10% SDS-PAGE and blotted onto nitrocellulose membrane. Ponceau staining was used to reveal equal protein loading and subsequent quantification. Blots were blocked with 5% (*v*/v) chicken egg yolk in TBST (20 mM Tris-HCl pH 8.0, 150 mM NaCl, 0.05% (*v*/v) Tween-20) for 1 h at room temperature. $K_{IR}2.1$ WT and mutants were detected by N-terminal $K_{IR}2.1$ antibody (Santa Cruz Biotechnology, Dallas Tx, USA, cat. No. sc-18708) and peroxidase-conjugated donkey anti-goat secondary antibody (Jackson ImmunoResearch, West Grove, PA, cat. No. 705-035-003) followed by ECL detection procedure (GE Healthcare, Hoevelaken, The Netherlands). For quantification purposes, untransfected HEK293T cells were used as blank and protein levels were normalized to ponceau staining levels. Differences between group averages were tested by using a one-way ANOVA with a Bonferroni's post-hoc test.

Immunofluorescence microscopy

HEK293T and MES-1 cells were cultured on pre-coated (0.1% gelatin) glass coverslips and transfected using Lipofectamin (Invitrogen, Breda, The Netherlands). Cell fixation, immunolabeling and imaging were performed exactly as described earlier [29]. Antibodies used were anti-$K_{IR}2.1$ (1:250; Santa Cruz Biotechnology, cat. no. sc-18708) and anti-Pan Cadherin (1:800, Sigma-Aldrich, St. Louis MO, USA, cat. No. C1821). HEK293T cells were imaged by confocal microscopy using a Zeiss LSM 700 confocal microscope (Carl Zeiss Microscopy GmbH, Germany) equipped with a 63× oil immersion objective (NA 1.4). Excitation was performed with an air-cooled Argon ion laser (LASOS, RMC 7812Z, 488 nm) for GFP and a HeNE (LASOS, SAN 7450A, 543 nm) laser for DyLight. MES-1 cells were imaged using a conventional Nikon eclipse 80i light microscopy equipped with a 40× objective (NA 0.75).

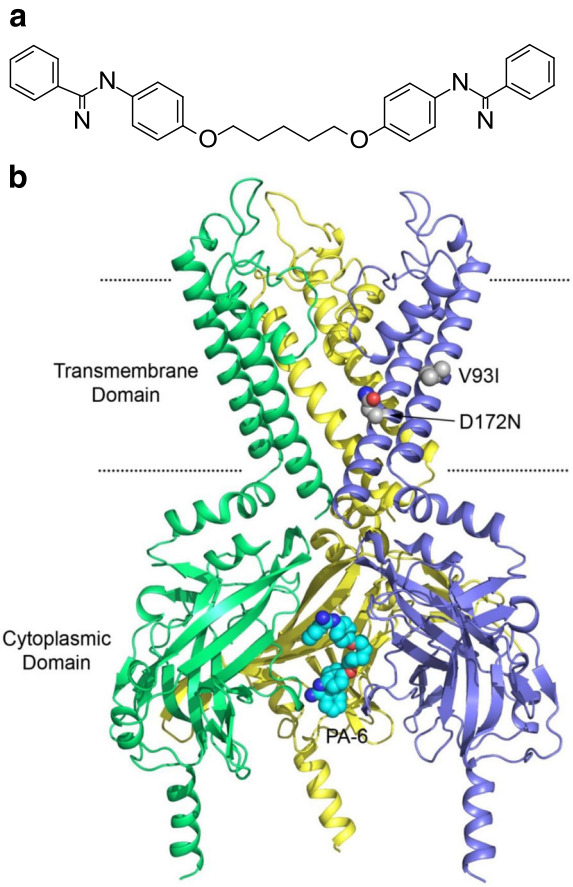

Fig. 1 **a** Chemical structure of PA-6 (drawn in Accelrys Draw 4.1). **b** Compound PA-6 docked into a homology model of $K_{IR}2.1$. Three subunits are shown in side view; the fourth is removed for clarity. The location of mutations V93I (M1 helix) and D172N (M2 helix) are depicted in spheres representation. PA-6, bound to the cytoplasmic domain, is shown as cyan spheres. Nitrogen atoms are coloured blue, oxygen atoms are shown in red. Approximate membrane boundaries are indicated as black dotted lines. The figure was generated with Pymol

Results

V93I and D172N mutations do not interfere with the PA-6 $K_{IR}2.1$ channel interaction

To determine whether V93I or D172N mutations in the $K_{IR}2.1$ channel may interfere with PA-6 current block,

mutations and PA-6 channel interaction were modelled. Figure 1b shows the docking result of PA-6 into the V93I/D172N double mutant homology model of $K_{IR}2.1$. The results demonstrate that these mutations are unlikely to influence binding of PA-6 to the previously identified binding site in the cytoplasmic domain [20]. Both mutations are located in the transmembrane domain and thus >30 Å away from the binding site.

PA-6 inhibits inward rectifier currents carried by V93I and D172N mutant $K_{IR}2.1$ channels

To determine the functional effects of PA-6 on the $K_{IR}2.1$ gain-of-function mutant channels, expression constructs were transiently transfected into HEK293T cells. Currents were measured in the inside-out mode, to allow for direct access of PA-6 to the cytoplasmic channel pore, of the patch-clamp technique using a ramp-protocol from −100 to +100 mV. PA-6 dose dependently inhibited inward rectifier inward (at −80 mV) and outward (at +50 mV) currents carried by WT, V93I and D172N $K_{IR}2.1$ channels (Fig. 2a). A small voltage dependency of block was observed for WT and both mutant channels as reflected in small, but not significant, changes in IC_{50} values obtained at −80 and +50 mV for each $K_{IR}2.1$ type. Interestingly, in contrast to WT and V93I, D172N outward current was less sensitive for PA-6 block than inward current. Whereas WT and V93I displayed virtually identical dose dependent block (IC_{50} of 52.9 and 58.0 nM at −80 mV and 35.5 and 43.6 nM at +50 mV for WT and V93I channels respectively), D172N channels were approximately two to three fold less sensitive (IC_{50} 109.3 nM at −80 mV and 128.9 nM at +50 mV) (Fig. 2b).

Using the whole cell mode of the patch clamp technique, gain-of-function of D172N mutant became apparent as a change in the rectification index ((1-(outward current at −40 mV divided by inward current at −100 mV)) [30], not correct for liquid junction potential) from 0.83 ± 0.11 (n = 9, mean ± s.d.) for WT channels to 0.70 ± 0.06 (n = 10, $P < 0.01$) in D172N channels (Fig. 3a), in accordance with earlier findings [2]. No change in rectification index of V93I (0.87 ± 0.09, n = 10, n.s.) was found. In addition, whereas PA-6 sensitivity was decreased in the whole cell mode, compared to the inside-out mode no differences were observed between WT and mutant channels (Fig. 3b). In the presence of 1 μM of PA-6, a non-significant (n.s.) reduction of outward I_{K1} at −50 mV by 28 ± 36%, 18 ± 20% and 10 ± 6%, for WT, V93I and D172N channels respectively was observed. At 3 μM, PA-6 significantly inhibited I_{K1} at −50 mV by 94 ± 6%

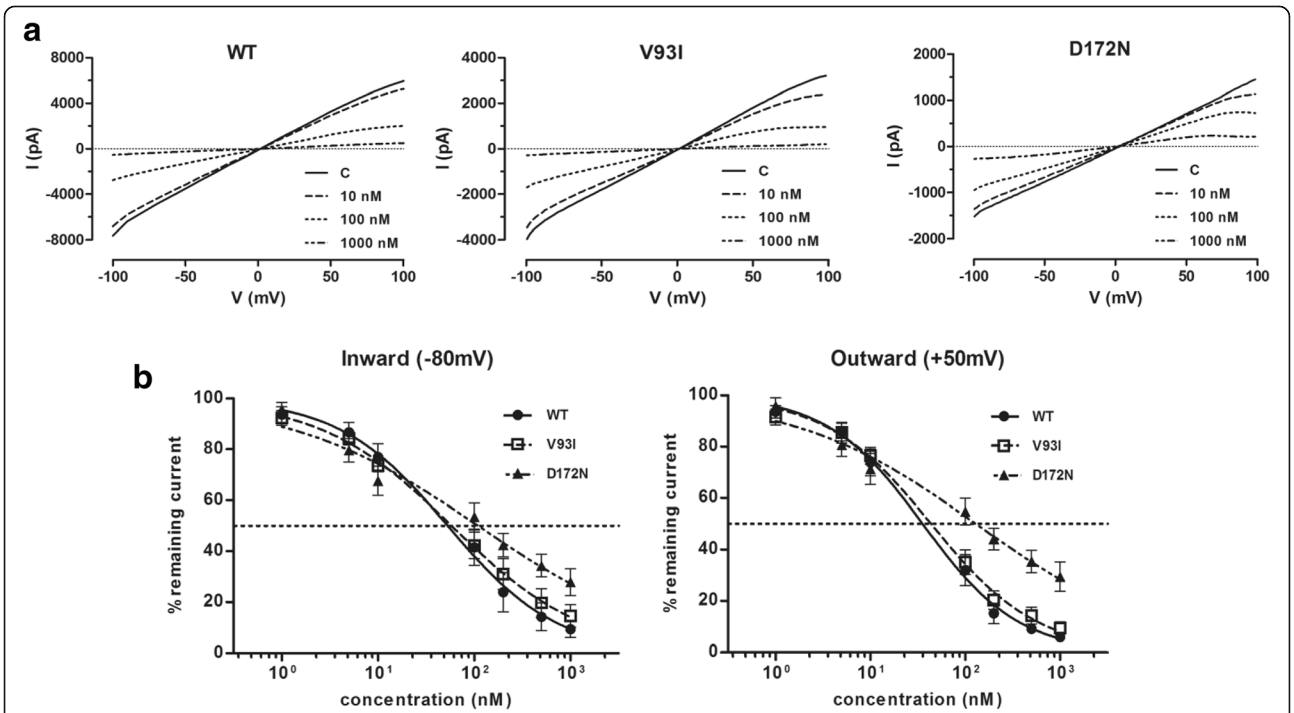

Fig. 2 PA-6 dose dependently inhibits I_{K1} currents carried by homotypic wild-type (WT), V93I and D172N $K_{IR}2.1$ channels measured in the inside out mode. **a** Steady state $K_{IR}2.1$ current traces from WT, V93I and D172N $K_{IR}2.1$ channel containing inside-out patches elicited by a voltage ramp protocol from −100 to 100 mV, under baseline conditions (C) and upon application of 10, 100 and 1000 nM of PA-6. Measurements were performed using symmetrical high potassium concentrations at both sides of the patch. **b** IC_{50} curves of PA-6 for the inward (at −80 mV) and outward (at +50 mV) $K_{IR}2.1$ currents of WT (n = 10), V93I (n = 9) and D172N (n = 11) channel containing patches. Error bars indicate s.e.m

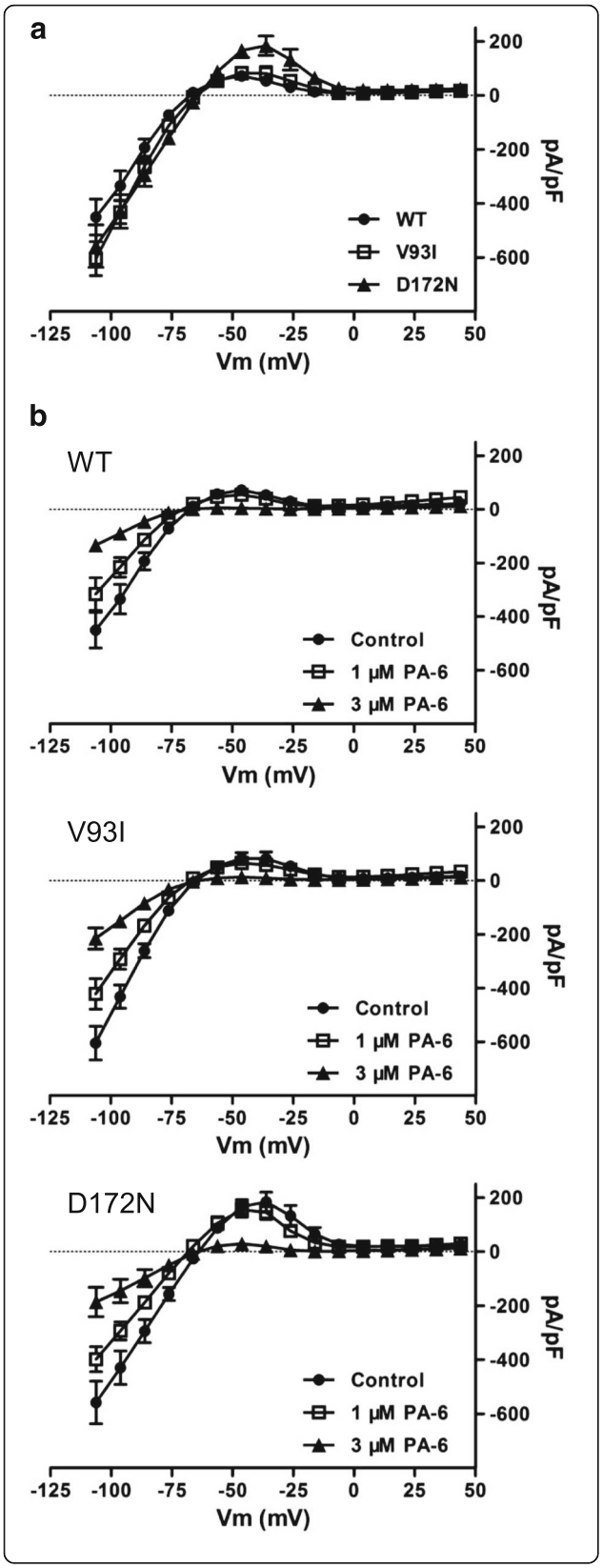

Fig. 3 PA-6 dose dependently inhibits I_{K1} currents carried by homotypic wild-type (WT), V93I and D172N $K_{IR}2.1$ channels in the whole cell mode. **a** Comparison of whole cell IV-curves obtained from HEK293 cells expressing WT (*closed circles*), V93I (*open squares*) or D172N (*closed triangles*) $K_{IR}2.1$ channels. Currents were elicited by 1 s test pulses ranging between −120 and +30 mV, in 10 mV increments and correct for liquid junction potential. **b** Whole cell steady state current IV-curves from WT, V93I and D172N $K_{IR}2.1$ channels expressed in HEK293 under control (*closed circles*), 1 μM PA-6 (*open squares*) and 3 μM PA-6 conditions. Voltage protocol as in panel **a**

($P < 0.05$), 77 ± 29% ($P < 0.05$) and 86 ± 7% ($P < 0.01$), for WT, V93I and D172N channels, respectively. For the inward current at −110 mV, 1 and 3 μM PA-6 inhibited I_{K1} by 30 ± 16% (n.s.) and 68 ± 15% ($P < 0.01$), 28 ± 14% ($P < 0.05$) and 64 ± 4% ($P < 0.001$), 30 ± 10% (n.s.) and 83 ± 1% ($P < 0.01$) for WT, V93I and D172N channels, respectively. We conclude that in the whole cell mode, PA-6 inhibits WT, V93I and D172N channels with similar efficacy resulting in IC_{50} values between 1 and 3 μM.

V93I and D172N mutations do not affect PA-6 mediated increase in $K_{IR}2.1$ expression and intracellular accumulation

When applied at concentrations of 10 μM, PA-6 is able to enhance expression of WT $K_{IR}2.1$ in cells stably expressing GFP-tagged $K_{IR}2.1$ [20]. To assess the effects of PA-6 on expression of WT and mutant channels in transiently transfected HEK293T cells, cultures were treated with 0, 0.2, 1 and 5 μM PA-6 for 24 h after which expression levels were detected by Western blot analysis. PA-6 treatment increased $K_{IR}2.1$ expression levels for all three variants (Fig. 4a). Strongest responses were obtained with 5 μM PA-6 added to the medium that reached significance for WT ($P < 0.001$) and V931 ($P < 0.01$) whereas a trend was observed for D172N ($P = 0.09$) (Fig. 4b). Lower concentrations of PA-6 did not result in significant increased expression.

To detect the subcellular location of the WT, V93I and D172N channels following PA-6 application, confocal immunofluorescent microscopy was performed in HEK293T cells. In non-treated control cells, both WT and mutant channels were mainly expressed at the plasma membrane, where they demonstrate colocalization with Cadherin (Fig. 5 left column), whereas PA-6 treatment (1 μM) for 24 h induced an intracellular increase of the channel proteins in small aggregates, irrespectively whether these are WT or mutant (Fig. 5, middle column). PA-6 treatment at 5 μM for 24 further increased the level of intracellular accumulation (Fig. 5, right column). To exclude any potential effect of cell-type specific response, immune detection was also performed in the mesoderm-like cell line MES-1 as shown previously [29] which yielded similar responses (Fig. 6). In control cells, WT and mutant channels were

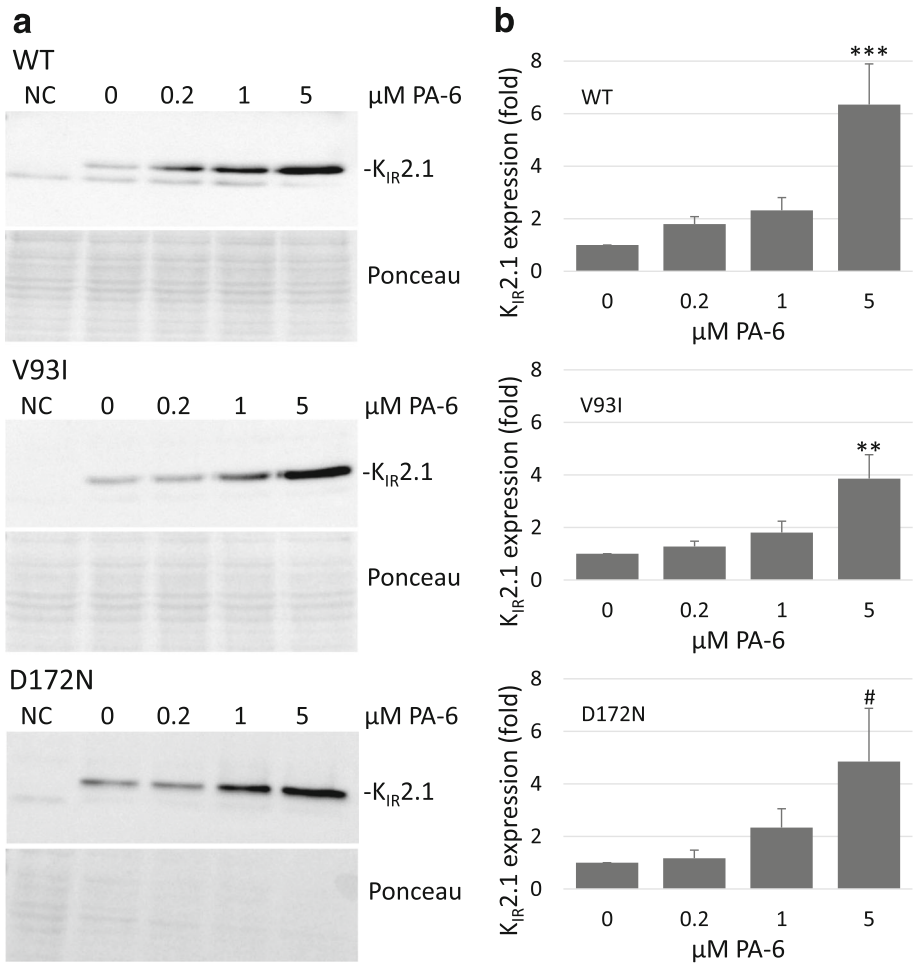

Fig. 4 PA-6 application for 24 h increases WT, V93I and D172N $K_{IR}2.1$ channel expression. **a** Dose-dependent (0-5 μM) effect of 24 h exposure to PA-6 on HEK293T cells transiently transfected with WT, V93I and D172N $K_{IR}2.1$ channels. NT indicates non-transfected cells. Ponceau staining was used as loading control for quantification (**b**) Summarized quantification data from WT (n = 11 independent western blots), V93I (n = 11) and D172N (n = 13) are shown in mean ± s.e.m. *** $P < 0.001$ vs. control, ** $P < 0.01$ vs. control, #$P = 0.09$ vs. control

localized mainly at the plasma membrane, whereas 5 μM of PA-6 (24 h) resulted in intracellular accumulation, in a fashion similar as for chloroquine although the latter treatment resulted in aggregates more equally in size [27, 31].

Discussion

Due to the high risk of sudden cardiac death, ICD implantation is indicated in congenital SQT patients. However, pharmacological treatment is warranted in young children not amenable for ICD implantation, in patients refusing an ICD and as a bridge to ICD therapy [10]. In congenital SQT patients, responsiveness of the QTc interval towards class IC and class III antiarrhythmics were unsatisfactory. SQT patients did not show anticipated responses to flecainide, d-sotalol or ibutilide [32, 33]. Only hydroquinidine was able to prolong QTc to borderline or normal duration [32, 33]. Short QT syndrome type 1 (SQT1) results from gain-of-function mutations in the $K_v11.1$ (hERG) channel encoded by the *KCNH2* gene, and is the best studied SQT subtype with respect to pharmacological treatment. The N588K gain-of-function mutation appears a hotspot in SQT1. Interestingly, N558K channels were less sensitive for Class III antiarrhythmics like d-sotalol [34], and E-4031 (11-fold) [11]. Accordingly, d-sotalol was unable to prolong the QT interval in SQT1 N558K patients [34]. In contrast, disopyramide (1.5-fold) and hydroquinidine (3.5-fold) displayed smaller differences in IC_{50} values for WT and N558K $K_v11.1$ channels, respectively. Clinical studies indeed showed favourable responses to hydroquinidine in SQT1 [33, 35], whereas QTc prolongation in non-$K_v11.1$ SQT patients was smaller [33]. The SQT2 associated mutation V307L in the $K_v7.1$ channel was shown to be equally sensitive for mefloquine as its WT variant, on

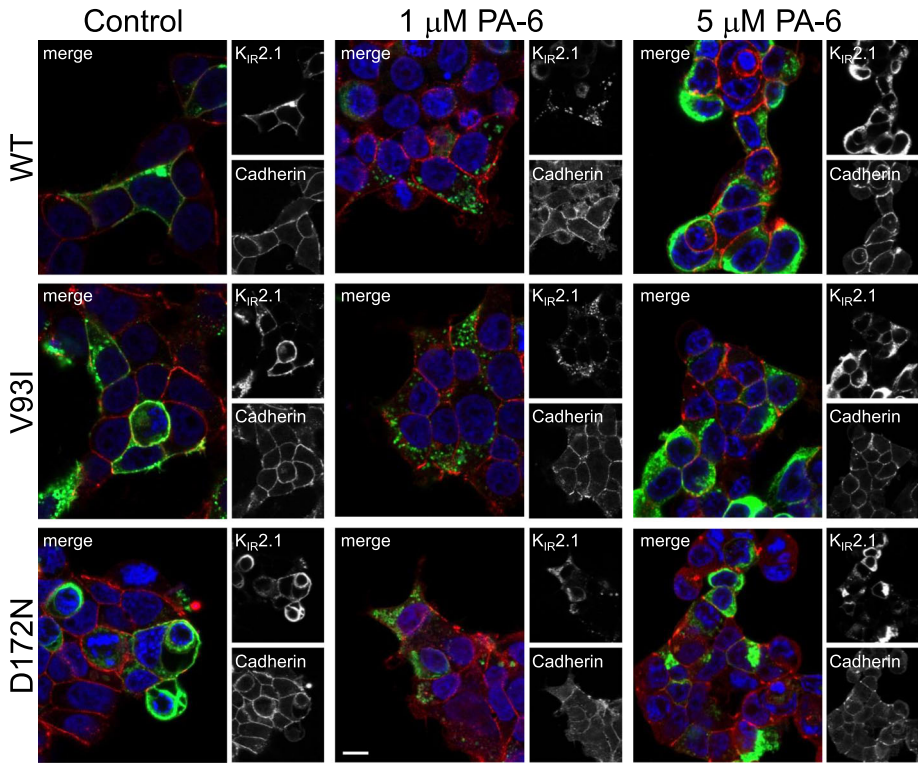

Fig. 5 PA-6 treatment for 24 h induces intracellular $K_{IR}2.1$ accumulation of WT, V93I and D172N channel proteins in HEK293T cells. Confocal microscopy optical slices (0.7-0.8 μm) displaying $K_{IR}2.1$ (*green*) localization in HEK293T cells transfected with WT, V93A and D172N channels under control conditions and following 24 h of PA-6 (1 and 5 μM). Cadherin (*red*) co-staining identifies the position of the plasma membrane. DAPI (*blue*) is used to visualize nuclei. Scale bars represent 10 μm

which basis the authors suggested that this drug may be an effective treatment strategy in this patient population [14]. Interestingly, the same V307L mutation increased the IC_{50} value for the $K_v7.1$ inhibitor Chromanol293B by 7-fold [36], indicating again that a mutation specific pharmacological approach is favourable. The SQT3 associated D172N mutation in $K_{IR}2.1$ was equally sensitive for chloroquine (1.2-3.3 μM) as its WT counterpart (1.4-2.4 μM) measured in the whole cell mode [12, 13]. Here we demonstrate that upon acute superfusion, PA-6 is also able to inhibit D172N mutant $K_{IR}2.1$ channel with an IC_{50} only two to three fold higher than that of WT channels, measured in the inside-out mode, and that potency of inhibition of the V93I channel was similar as for WT. In the whole cell mode, acute PA-6 superfusion inhibits WT, V93I and D172N with similar efficacy. Therefore, PA-6 could potentially be effective in addressing SQT3 and AF associated with each of these two mutations.

In contrast to PA-6, chloroquine suffers from lack of specificity as it significantly inhibits delayed rectifier (I_{Kr}), sodium (I_{Na}) and l-type calcium ($I_{Ca\text{-}l}$) currents [20, 37]. Upon long-term exposure however, both chloroquine and PA-6 are able to increase $K_{IR}2.1$ channel expression [20, 27, 31, 38]. However, due to its lower potency, the concentrations at which chloroquine affected trafficking (5 μM) are slightly closer to its IC_{50} for acute blockade than seen for PA-6. Furthermore, the majority of PA-6 induced increase of $K_{IR}2.1$ channel expression as detected by Western blot upon chronic exposure results from intracellular accumulation instead of functional channels at the plasma membrane.

The acute channel inhibiting effect of a drug may or may be not be correlated with its chronic effect on ion channel expression. For example, pentamidine inhibits the $K_{IR}2.1$ channel acutely and decreases $K_{IR}2.1$ expression upon chronic treatment [38, 39], but its structural derivative PA-6 inhibits $K_{IR}2.1$ currents acutely while it increases channel expression chronically as shown here and previously [20]. In the former case, both drug effects are additive and maybe synergistic. In the case of PA-6, acute and chronic effects are opposite, but at 1 and 3 μM, the acute effects on current inhibition are stronger than the increases in channel expression levels upon chronic exposure. Only upon acute termination of PA-6 application, the effects on expression may temporarily prevail over the acute blocking effect (or absence thereof) resulting in enhanced I_{K1}.

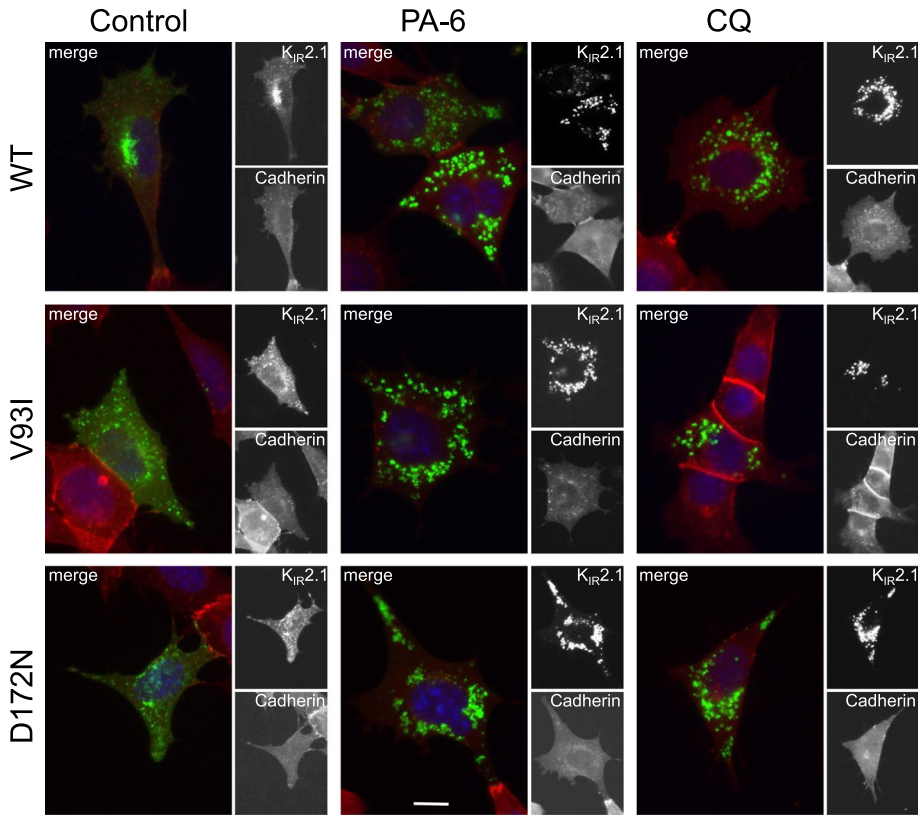

Fig. 6 PA-6 treatment for 24 h induces intracellular $K_{IR}2.1$ accumulation of WT, V93I and D172N channel proteins in MES-1 cells. Whole cell $K_{IR}2.1$ (*green*) and Cadherin (*red*) localization in MES-1 cells transfected with WT, V93I or D172N channels in non-treated (control), PA-6 (5 μM, 24 h) or chloroquine (10 μM, 24 h) conditions imaged by conventional fluorescent microscopy. DAPI (*blue*) was used to identify nuclei. Scale bars represent 10 μm

Limitations

The effects of PA-6 on WT, V93I and D172N $K_{IR}2.1$ channels have only been tested in ectopic expression systems and therefore the effects of their blockade on cardiac action potential characteristics could not be evaluated.

Conclusions

In the $K_{IR}2.1$ ion channel, V93I and D172N gain-of-function mutations do not blunt the inhibitory capacity of PA-6. PA-6 application results in enhanced $K_{IR}2.1$ protein expression, mainly localized in intracellular aggregates. From our findings presented here, we conclude that PA-6 may be considered for further preclinical evaluation for treatment of congenital SQT3 and AF.

Abbreviations

AF: Atrial fibrillation; GFP: Green fluorescent protein; HEK: Human embryonal kidney; $I_{Ca\text{-}L}$: L-type Calcium current; ICD: Implantable cardioverter-defibrillator; I_{K1}: Inward rectifier potassium current; I_{KACh}: Acetylcholine activated inward rectifier potassium current; I_{Kr}: Delayed rectifier current; I_{Na}: Sodium current; PA-6: Pentamidine analogue-6; SQTx: Short QT syndrome type x; WT: Wild-type

Acknowledgements

Y.J. is the recipient of a scholarship from the Chinese Scholarship Council. We thank Drs. M.B. Rook and T.P. de Boer (Dept of Medical Physiology, University Medical Center Utrecht, The Netheralands) for fruitful discussions on electrophysiological measurements, and Dr. I.S. Grigoriev (Dept. of Cell Biology, Utrecht University, The Netherlands) for technical assistance concerning confocal microscopy.

Funding

This work was supported by the Chinese Scholarship Council (CSC).

Availability of data and materials

Not applicable.

Authors' contributions

YJ, MGV, HT and MJCH performed electrophysiological recordings; KD, GvH generated V93I and D172N expression constructs; EMZP and ASW performed and analyzed molecular modelling; JZ performed and analyzed western blot experiments; FLR and MAGvdH performed and analyzed the subcellular localization experiments; MAGvdH and YJ designed the study. YJ, MAGvdH, GvH and ASW wrote the manuscript. All authors read and approved the manuscript.

Ethics approval and consent to participate

Not applicable.

Consent for publication

Not applicable.

Competing interests
The authors declare that they have no competing interest.

Publisher's Note
Springer Nature remains neutral with regard to jurisdictional claims in published maps and institutional affiliations.

Author details
[1]Department of Medical Physiology, Division of Heart and Lungs, University Medical Center Utrecht, Yalelaan 50, 3584 CM Utrecht, The Netherlands. [2]Center for Molecular Medicine, Department of Medical Genetics, University Medical Center Utrecht, Utrecht, The Netherlands. [3]Department of Pharmacology and Toxicology, University of Vienna, Vienna, Austria.

Received: 26 April 2017 Accepted: 11 July 2017
Published online: 15 July 2017

References

1. Hibino H, Inanobe A, Furutani K, Murakami S, Findlay I, Kurachi Y. Inwardly rectifying potassium channels: their structure, function, and physiological roles. Physiol Rev. 2010;90:291–366.
2. Priori SG, Pandit SV, Rivolta I, Berenfeld O, Ronchetti E, Dhamoon A, Napolitano C, Anumonwo J, di Barletta MR, Gudapakkam S, Bosi G, Stramba-Badiale M, Jalife J. A novel form of short QT syndrome (SQT3) is caused by a mutation in the KCNJ2 gene. Circ Res. 2005;96:800–7.
3. Ambrosini E, Sicca F, Brignone MS, D'Adamo MC, Napolitano C, Servettini I, Moro F, Ruan Y, Guglielmi L, Pieroni S, Servillo G, Lanciotti A, Valvo G, Catacuzzeno L, Franciolini F, Molinari P, Marchese M, Grottesi A, Guerrini R, Santorelli FM, Priori S, Pessia M. Genetically induced dysfunctions of Kir2.1 channels: implications for short QT3 syndrome and autism-epilepsy phenotype. Hum Mol Genet. 2014;23:4875–86.
4. Xia M, Jin Q, Bendahhou S, He Y, Larroque MM, Chen Y, Zhou Q, Yang Y, Liu Y, Liu B, Zhu Q, Zhou Y, Lin J, Liang B, Li L, Dong X, Pan Z, Wang R, Wan H, Qiu W, Xu W, Eurlings P, Barhanin J, Chen Y. Kir2.1 gain-of-function mutation underlies familial atrial fibrillation. Biochem Biophys Res Commun. 2005;332:1012–9.
5. Deo M, Ruan Y, Pandit SV, Shah K, Berenfeld O, Blaufox A, Cerrone M, Noujaim SF, Denegri M, Jalife J, Priori SG. KCNJ2 mutation in short QT syndrome 3 results in atrial fibrillation and ventricular proarrhythmia. Proc Natl Acad Sci U S A. 2013;110:4291–6.
6. Hattori T, Makiyama T, Akao M, Ehara E, Ohno S, Iguchi M, Nishio Y, Sasaki K, Itoh H, Yokode M, Kita T, Horie M, Kimura T. A novel gain-of-function KCNJ2 mutation associated with short-QT syndrome impairs inward rectification of Kir2.1 currents. Cardiovasc Res. 2012;93:666–73.
7. Priori SG, Wilde AA, Horie M, Cho Y, Behr ER, Berul C, Blom N, Brugada J, Chiang CE, Huikuri H, Kannankeril P, Krahn A, Leenhardt A, Moss A, Schwartz PJ, Shimizu W, Tomaselli G, Tracy C. HRS/EHRA/APHRS expert consensus statement on the diagnosis and management of patients with inherited primary arrhythmia syndromes: document endorsed by HRS, EHRA, and APHRS in May 2013 and by ACCF, AHA, PACES, and AEPC in June 2013. Heart Rhythm. 2013;10:1932–63.
8. Patel C, Yan GX, Antzelevitch C. Short QT syndrome: from bench to bedside. Circ Arrhythm Electrophysiol. 2010;3:401–8.
9. Pérez Riera AR, Paixão-Almeida A, Barbosa-Barros R, Yanowitz FG, Baranchuk A, Dubner S, Palandri Chagas AC. Congenital short QT syndrome: landmarks of the newest arrhythmogenic cardiac channelopathy. Cardiol J. 2013;20:464–71.
10. Patel C, Antzelevitch C. Pharmacological approach to the treatment of long and short QT syndromes. Pharmacol Ther. 2008;118:138–51.
11. McPate MJ, Duncan RS, Witchel HJ, Hancox JC. Disopyramide is an effective inhibitor of mutant HERG K^+ channels involved in variant 1 short QT syndrome. J Mol Cell Cardiol. 2006;41:563–6.
12. El Harchi A, McPate MJ, Zhang YH, Zhang H, Hancox JC. Action potential clamp and chloroquine sensitivity of mutant Kir2.1 channels responsible for variant 3 short QT syndrome. J Mol Cell Cardiol. 2009;47:743–7.
13. Lopez-Izquierdo A, Ponce-Balbuena D, Ferrer T, Sachse FB, Tristani-Firouzi M, Sanchez-Chapula JA. Chloroquine blocks a mutant Kir2.1 channel responsible for short QT syndrome and normalizes repolarization properties in silico. Cell Physiol Biochem. 2009;24:153–60.
14. El Harchi A, McPate MJ, Zhang YH, Zhang H, Hancox JC. Action potential clamp and mefloquine sensitivity of recombinant 'I_{KS}' channels incorporating the V307L KCNQ1 mutation. J Physiol Pharmacol. 2010;61:123–31.
15. Camm AJ, Lip GY, De Caterina R, Savelieva I, Atar D, Hohnloser SH, Hindricks G, Kirchhof P, ESC Committee for Practice Guidelines (CPG). 2012 focused update of the ESC guidelines for the management of atrial fibrillation: an update of the 2010 ESC guidelines for the management of atrial fibrillation. Developed with the special contribution of the European Heart Rhythm Association. Eur Heart J. 2012;33:2719–47.
16. Workman AJ, Smith GL, Rankin AC. Mechanisms of termination and prevention of atrial fibrillation by drug therapy. Pharmacol Ther. 2011;131:221–41.
17. Ehrlich JR, Nattel S. Novel approaches for pharmacological management of atrial fibrillation. Drugs. 2009;69:757–74.
18. Noujaim SF, Stuckey JA, Ponce-Balbuena D, Ferrer-Villada T, López-Izquierdo A, Pandit S, Calvo CJ, Grzeda KR, Berenfeld O, Chapula JA, Jalife J. Specific residues of the cytoplasmic domains of cardiac inward rectifier potassium channels are effective antifibrillatory targets. FASEB J. 2010;24:4302–12.
19. Filgueiras-Rama D, Martins RP, Mironov S, Yamazaki M, Calvo CJ, Ennis SR, Bandaru K, Noujaim SF, Kalifa J, Berenfeld O, Jalife J. Chloroquine terminates stretch-induced atrial fibrillation more effectively than flecainide in the sheep heart. Circ Arrhythm Electrophysiol. 2012;5:561–70.
20. Takanari H, Nalos L, Stary-Weinzinger A, de Git KC, Varkevisser R, Linder T, Houtman MJ, Peschar M, de Boer TP, Tidwell RR, Rook MB, Vos MA, van der Heyden MAG. Efficient and specific cardiac I_{K1} inhibition by a new pentamidine analogue. Cardiovasc Res. 2013;99:203–14.
21. Ji Y, Varkevisser R, Opacic D, Bossu A, Kuiper M, Beekman JDM, Yang S, Khan AP, Dobrev D, Voigt N, Wang MZ, Verheule S, Vos MA, Van der Heyden MAG. The inward rectifier current inhibitor PA-6 terminates atrial fibrillation and does not cause ventricular arrhythmias in dedicated goat and dog models. Br J Pharmacol. 2017; doi:10.1111/bph.13869.
22. Varkevisser R, Houtman MJ, Linder T, de Git KC, Beekman HD, Tidwell RR, IJzerman AP, Stary-Weinzinger A, Vos MA, van der Heyden MAG. Structure-activity relationships of pentamidine-affected ion channel trafficking and dofetilide mediated rescue. Br J Pharmacol. 2013;169:1322–34.
23. Zhou Z, Gong Q, January CT. Correction of defective protein trafficking of a mutant HERG potassium channel in human long QT syndrome. Pharmacological and temperature effects. J Biol Chem. 1999;274:31123–6.
24. Smith JL, Reloj AR, Nataraj PS, Bartos DC, Schroder EA, Moss AJ, Ohno S, Horie M, Anderson CL, January CT, Delisle BP. Pharmacological correction of long QT-linked mutations in KCNH2 (hERG) increases the trafficking of Kv11.1 channels stored in the transitional endoplasmic reticulum. Am J Physiol Cell Physiol. 2013;305:C919–30.
25. Anderson CL, Kuzmicki CE, Childs RR, Hintz CJ, Delisle BP, January CT. Large-scale mutational analysis of K_v11.1 reveals molecular insights into type 2 long QT syndrome. Nat Commun. 2014;5:5535.
26. Guex N, Peitsch MC. SWISS-MODEL and the Swiss-PdbViewer: an environment for comparative protein modeling. Electrophoresis. 1997;18:2714–23.
27. Jansen JA, de Boer TP, Wolswinkel R, van Veen TA, Vos MA, van Rijen HV, van der Heyden MAG. Lysosome mediated Kir2.1 breakdown directly influences inward rectifier current density. Biochem Biophys Res Commun. 2008;367:687–92.
28. Houtman MJ, Takanari H, Kok BG, van Eck M, Montagne DR, Vos MA, de Boer TP, van der Heyden MAG. Experimental mapping of the canine KCNJ2 and KCNJ12 gene structures and functional analysis of the canine K_{IR}2.2 ion channel. Front Physiol. 2012;3:9.
29. Ji Y, Takanari H, Qile M, Nalos L, Houtman MJC, Romunde FL, Heukers R, Van Bergen en Henegouwen PMP, Vos MA, Van der Heyden MAG. Class III antiarrhythmic drugs amiodarone and dronedarone impair KIR2.1 backward trafficking. J Cell Mol Med. 2017; doi:10.1111/jcmm.13172.
30. Anumonwo JMB. Biophysical properties of inward rectifier potassium channels. In: Zipes D, Jalife J, editors. Cardiac electrophysiology: from cell to bedside. Philadelphia: Saunders; 2004. p. 112–9.
31. Varkevisser R, Houtman MJ, Waasdorp M, Man JC, Heukers R, Takanari H, Tieland RG, van Bergen En Henegouwen PM, Vos MA, van der Heyden MAG. Inhibiting the clathrin-mediated endocytosis pathway rescues KIR2.1 downregulation by pentamidine. Pflugers Arch 2013;465:247-259.
32. Gaita F, Giustetto C, Bianchi F, Schimpf R, Haissaguerre M, Calò L, Brugada R, Antzelevitch C, Borggrefe M, Wolpert C. Short QT syndrome: pharmacological treatment. J Am Coll Cardiol. 2004;43:1494–9.
33. Giustetto C, Schimpf R, Mazzanti A, Scrocco C, Maury P, Anttonen O, Probst V, Blanc JJ, Sbragia P, Dalmasso P, Borggrefe M, Gaita F. Long-term follow-up of patients with short QT syndrome. J Am Coll Cardiol. 2011;58:587–95.
34. Brugada R, Hong K, Dumaine R, Cordeiro J, Gaita F, Borggrefe M, Menendez TM, Brugada J, Pollevick GD, Wolpert C, Burashnikov E, Matsuo K, Wu YS,

Guerchicoff A, Bianchi F, Giustetto C, Schimpf R, Brugada P, Antzelevitch C. Sudden death associated with short-QT syndrome linked to mutations in HERG. Circulation. 2004;109:30–5.
35. Pirro E, De Francia S, Banaudi E, Riggi C, De Martino F, Piccione FM, Giustetto C, Racca S, Agnoletti G, Di Carlo F. Short QT syndrome in infancy. Therapeutic drug monitoring of hydroquinidine in a newborn infant. Br J Clin Pharmacol. 2011;72:982–4.
36. Lerche C, Bruhova I, Lerche H, Steinmeyer K, Wei AD, Strutz-Seebohm N, Lang F, Busch AE, Zhorov BS, Seebohm G. Chromanol 293B binding in KCNQ1 (Kv7.1) channels involves electrostatic interactions with a potassium ion in the selectivity filter. Mol Pharmacol. 2007;71:1503–11.
37. Sánchez-Chapula JA, Salinas-Stefanon E, Torres-Jácome J, Benavides-Haro DE, Navarro-Polanco RA. Blockade of currents by the antimalarial drug chloroquine in feline ventricular myocytes. J Pharmacol Exp Ther. 2001;297:437–45.
38. Nalos L, de Boer TP, Houtman MJ, Rook MB, Vos MA, van der Heyden MAG. Inhibition of lysosomal degradation rescues pentamidine-mediated decreases of $K_{IR}2.1$ ion channel expression but not that of $K_v11.1$. Eur J Pharmacol. 2011; 652:96–103.
39. De Boer TP, Nalos L, Stary A, Kok B, Houtman MJ, Antoons G, van Veen TA, Beekman JD, de Groot BL, Opthof T, Rook MB, Vos MA, van der Heyden MA. The anti-protozoal drug pentamidine blocks $K_{IR}2.x$-mediated inward rectifier current by entering the cytoplasmic pore region of the channel. Br J Pharmacol. 2010;159:1532–41.